Development 129, 5827-5838
© 2002 The Company of Biologists Ltd
doi:10.1242/dev.00164

DEVELOPMENT AND DISEASE

Dishevelled 2 is essential for cardiac outflow tract development, somite segmentation and neural tube closure

Natasha S. Hamblet[1,2,3], Nardos Lijam[3], Pilar Ruiz-Lozano[2], Jianbo Wang[1,2], Yasheng Yang[4], Zhenge Luo[5], Lin Mei[5], Kenneth R. Chien[2], Daniel J. Sussman[4] and Anthony Wynshaw-Boris[1,2,3,*]

[1]Departments of Pediatrics and Medicine, UCSD Comprehensive Cancer Center, University of California, San Diego, 9500 Gilman Drive, La Jolla, CA 92093-0627, USA
[2]Institute of Molecular Medicine, University of California, San Diego, 9500 Gilman Drive, La Jolla, CA 92093-0641, USA
[3]Genetic Disease Research Branch, National Human Genome Research Institute, National Institutes of Health, Bethesda, MD 20814, USA
[4]University of Maryland School of Pharmacy, Department of Pharmaceutical Sciences, 20 N. Pine Street, Baltimore, MD 21201, USA
[5]Departments of Neurobiology, Pathology, and Physical Medicine and Rehabilitation, University of Alabama at Birmingham, 1530 Third Avenue South, Birmingham, AL 35294-0021, USA
*Author for correspondence (e-mail: awynshawboris@ucsd.edu)

Accepted 19 September 2002

SUMMARY

The murine dishevelled 2 (*Dvl2*) gene is an ortholog of the *Drosophila* segment polarity gene *Dishevelled*, a member of the highly conserved Wingless/Wnt developmental pathway. *Dvl2*-deficient mice were produced to determine the role of *Dvl2* in mammalian development. Mice containing null mutations in *Dvl2* present with 50% lethality in both inbred 129S6 and in a hybrid 129S6-NIH Black Swiss background because of severe cardiovascular outflow tract defects, including double outlet right ventricle, transposition of the great arteries and persistent truncus arteriosis. The majority of the surviving *Dvl2*$^{-/-}$ mice were female, suggesting that penetrance was influenced by sex. Expression of *Pitx2* and plexin A2 was attenuated in *Dvl2* null mutants, suggesting a defect in cardiac neural crest development during outflow tract formation. In addition, ~90% of *Dvl2*$^{-/-}$ mice have vertebral and rib malformations that affect the proximal as well as the distal parts of the ribs. These skeletal abnormalities were more pronounced in mice deficient for both *Dvl1* and *Dvl2*. Somite differentiation markers used to analyze *Dvl2*$^{-/-}$ and *Dvl1*$^{-/-}$;*Dvl2*$^{-/-}$ mutant embryos revealed mildly aberrant expression of *Uncx4.1*, delta 1 and myogenin, suggesting defects in somite segmentation. Finally, 2-3% of *Dvl2*$^{-/-}$ embryos displayed thoracic spina bifida, while virtually all *Dvl1/2* double mutant embryos displayed cranioracchisisis, a completely open neural tube from the midbrain to the tail. Thus, *Dvl2* is essential for normal cardiac morphogenesis, somite segmentation and neural tube closure, and there is functional redundancy between *Dvl1* and *Dvl2* in some phenotypes.

Key words: *Dvl2*, Cardiac neural crest, DORV, PTA, Somitogenesis, Neural tube closure

INTRODUCTION

Dishevelled (*dsh* in *Drosophila* or *Dvl1* in mice) is a member of the conserved Wg/Wnt developmental pathway (Klingensmith et al., 1994; Theisen et al., 1994). Wg/Wnt proteins regulate cell fate and subsequent cell behavior (Bejsovec and Arias, 1991; Cadigan and Nusse, 1997; Moon et al., 1997). At least 18 different Wnts have been identified in humans but only three dishevelled genes (*Dvl1*, *Dvl2* and *Dvl3*) have been found in both humans and mice (Sussman et al., 1994; Klingensmith et al., 1996; Tsang et al., 1996; Lijam and Sussman, 1996; Yang et al., 1996; Semenov and Snyder, 1997). All of the dishevelled proteins contain three highly conserved motifs. The N-terminal DIX domain is involved in regulating the Wnt signal via binding to axin (Zeng et al., 1997; Smalley et al., 1999; Kishida et al., 1999). An internal PDZ (or GLGF/DHR) domain in all Dvl proteins is present in many diverse membrane associated proteins, suggesting a role in cell-cell communication (Ponting et al., 1997). Finally, a DEP domain present at the C terminus is found in many G-coupled proteins. In addition, Dvl2 is the only Dvl protein that contains a proline rich SH3-binding domain. The significance of this domain is unknown. The DIX domain and N-terminal region of the DEP domain are necessary to activate the canonical Wnt pathway to mediate dorsoventral (DV) and anteroposterior (AP) patterning, as well as cell fate determination. By contrast, the PDZ domain and C-terminal part of the DEP domain are implicated in the planar cell polarity pathway (PCP) in fly to

control the polarity of epithelial cells in the plane orthogonal to their apicobasal axis (Axelrod et al., 1998; Boutros et al., 1998; Moriguchi et al., 1999). Overexpression analysis in *Xenopus* has implicated these two domains, and most likely the PCP pathway, in the control of the convergent extension morphogenetic movements (Wallingford et al., 2000; Wallingford and Harland, 2001). Although functional significance can be assigned to each of these conserved motifs, the exact biochemical role of *Dishevelled* in transducing the Wnt signal is unknown. At present no human diseases have been linked to defects in *DVL1*, *DVL2* or *DVL3*.

The similarity between *dsh* mutants and the *wg* phenotype in *Drosophila* (Perrimon and Mahowald, 1987) indicates that an overlap in phenotype might be expected between *Wnt* mutants and Dvl knockout mice. All three of the murine *Dishevelled* genes are widely expressed in embryonic and adult tissues suggesting that there may be functional redundancy among the three genes. These findings make it difficult a priori to predict specific classes of defects that may occur in mammals after disruption of each of these genes. Surprisingly, null mutants for *Dvl1* exhibit deficits in social interaction and sensorimotor gating (Lijam et al., 1997). By contrast, mouse mutants that contain null mutations in *Wnt* genes result in mice with varied brain and developmental abnormalities (Cadigan and Nusse, 1997). For example, mice that are deficient in *Wnt1* display midbrain and hindbrain (cerebellar) abnormalities (McMahon and Bradley, 1990; Thomas and Capecchi, 1990), and *Wnt1/Wnt3a* double mutants have additional deficiencies in the neural crest (Ikeya et al., 1997). The neural crest is a migratory group of cells that emanate from the dorsal neural tube and give rise to various cell populations, including melanocytes, the dorsal root ganglia and the cardiac neural crest. Cardiac neural crest cells originate from the occipital neural tube and aid in septation of the outflow tracts and in aortic arch development.

The murine *Dvl1* and *Dvl2* genes are 64% identical and it is unknown whether *Dvl2* has a similar role as *Dvl1* in development. To address this question and to define further the role of individual *Dishevelled* genes in mammalian development, mice were generated that were deficient in *Dvl2*. We found that *Dvl2* is essential for normal cardiac morphogenesis, somite segmentation, and neural tube closure. In addition, there is functional redundancy between *Dvl1*and *Dvl2* in somite development and neural tube closure, as *Dvl1/2* double mutants display more severe defects than the *Dvl2* single mutants.

MATERIALS AND METHODS

Targeted disruption and generation of *Dvl2* deficient mice

A *Dvl2* genomic clone was isolated from a mouse strain 129 genomic DNA library in λ FIX II (Stratagene) as previously described (Yang et al., 1996). The 3 kb *Bgl*II fragment containing most of intron 1 and part of exon 2 was cloned in the *Bam*HI site of pPNT (Tybulewicz et al., 1991) in an orientation opposite to that of the direction of transcription of the *neo* marker to generate pPNT-*Bgl*I. The 4 kb *Hin*dIII fragment spanning exons 8 to half of 15 was first cloned in the *Hin*dIII site of pBluescript KS (Stratagene) and excised as a *Not*I/*Xho*I fragment for cloning into the *Not*I/*Xho*I sites of pPNT-BglII. The final construct, pPNT-Dvl2, has the *neo* gene interrupting the *Dvl2*-coding sequence at amino acid 71 (the *Bgl*II site in exon 2) and deleting exons 3-6 (the *Hin*dIII site in intron 6). Knockout mice were produced by gene targeting in TC1 embryonic stem (ES) cells (Deng et al., 1996). ES cell genotyping was performed by Southern blotting using a flanking probe and *Bam*HI/*Eco*RI double digestion with [^{32}P]dCTP random primed radiolabeled probe (High Prime-Boehringer Mannheim) and five clones were correctly targeted. Three of these clones were injected and all gave high frequency germline transmission. Lines were established in inbred 129S6 and mixed lines of 129S6 × NIH Black Swiss, as previously described (Deng et al., 1996). Genotyping for subsequent studies was by PCR using genomic tail DNA from adult animals and DNA extracted from yolk sac for early gestation embryos. The PCR primers were as follows: Dvl2/15 forward primer in exon 5, 5′-AGCAGTGCCTCCCGCCTCCTCA; Dvl2/16 reverse primer in exon 7, 5′-CCCATCACCACGCTC-GTTACTTTG; NLpgk *neo* forward primer, 5′-AGGCTTACC-CGCTTCCATTGCTCA. All animal experiments were carried out under protocols approved by the NHGRI/NIH and UCSD Animal Care and Use Committees and following NIH guidelines.

Immunoblot analysis

Brain tissue (0.2 mg) from wild-type and *Dvl2*$^{-/-}$ mice was homogenized in 1 ml of RIPA buffer containing Pefabloc (Boehringer Mannheim). Homogenates were subjected to centrifugation for 1 minute at full speed in a microcentrifuge. An aliquot of the supernatants was saved for A280 measurement (for normalization of gel loading), while the remainder was mixed with an equal volume of 2× SDS gel loading buffer and boiled for 3 minutes. Aliquots (20 μl) were loaded on a 7.5% polyacrylamide SDS minigel and subjected to electrophoresis and transfer to nitrocellulose membrane for western blot analysis. A polyclonal antibody to the C terminus of Dvl1 (Luo et al., 2002) and monoclonal antibodies to the C terminus of Dvl2 (2-10B5) (Song et al., 2000) and Dvl3 (3-4D3) (Strovel and Sussman, 1999) were used in conjunction with peroxidase-conjugated anti-mouse IgG (Sigma) for chemiluminescent detection (Amersham Pharmacia Biotech).

Scanning electron microscopy

Embryo hearts were collected at 18.5 dpc or embryos were collected at 8.5-10.5 dpc and fixed in 3% aldehyde solution (1.5% paraformaldehyde, 1.5% glutaraldehyde) in 0.1 M phosphate buffer pH 7.5, dehydrated in a graded ethanol series, then stored in 100% ethanol until scanning. Samples were critically point dried, mounted and then coated with 300 Angstrom gold-palladium. Specimens were viewed and photographed with a Cambridge Instrument Stereoscan 360 scanning electron microscope (Scripps Institute of Oceanography Analytical Facility).

Whole-mount in situ hybridization

Embryos were prepared for in situ using the protocol detailed by Wilkinson (Wilkinson, 1992) with modifications. Embryos were dissected at the appropriate ages, fixed in 4% paraformaldehyde in PBS then dehydrated in a methanol series. Embryos were rehydrated in PBT (0.01% Tween-20 in PBS), treated with 6% H_2O_2 to remove endogenous peroxidases and then permeabilized with proteinase K. Hybridization was performed at 70°C overnight in hybridization solution (50% formamide, 5×SSC pH 4.5, 50 μg/ml yeast tRNA, 1% SDS, 50 μg/ml heparin) using an RNA probe labeled with digoxigenin-UTP (Boehringer/Mannheim). Afterwards embryos were washed extensively in TBST (TBS with 0.1% Tween-20, Sigma) and blocked in 1% sheep serum in TBST. Transcripts were detected with anti-dig Fab′ conjugated with alkaline phosphatase followed by color reaction with X-phosphate/NBT substrate. Reactions were stopped with PBT and embryos stored in 80% glycerol/PBT until photographed.

Histology

Tissues were dissected and placed in 20 volumes of 10% buffered

formalin, dehydrated, embedded in paraffin wax, sectioned at 8 μM and stained by routine methods at the UCSD Histology Core. Photographs were taken using a Leica DMR light microscope mounted with a Spot 2 camera.

Bone and cartilage stain

Differential staining of mouse fetuses was carried out according to the procedure of McLeod (McLeod, 1980). Embryonic 17 and 18 dpc fetuses were skinned and eviscerated, fixed in a 95% ethanol solution for 5 days, then treated in acetone for 4 days to remove fat. Fetuses were stained with 0.3% Alcian Blue, 0.1% Alizarin Red S ethanol/acetic acid solution for 3 days followed by clearing in a graded series of glycerol/1% KOH (20-80% glycerol, 1 week each step). Skeletons were stored in 100% glycerol and photographed using a Leica dissection microscope and Spot 2 camera.

RESULTS

Generation of *Dvl2*-deficient mice

To produce mice that contain a null allele for *Dvl2*, part of exon 2 and all of exons 3-6 were disrupted by the insertion of PGKneo (Fig. 1A), replacing approximately 1.2 kb of the *Dvl2*-coding region and introducing multiple stop codons from PGKneo 3′ into exon 2. Targeting was performed in TC1 ES cells and five targeted clones were identified by Southern blot screening (Fig. 1B, lanes 2-6). This mutant allele was established in the germline from two separate clones in both mixed (129S6×NIH Black Swiss) and uniform (129S6) genetic backgrounds, demonstrated by southern blotting of newborn tail DNA (Fig. 1C). Homozygous, heterozygous and wild-type offspring were observed in F_2 litters in both backgrounds. Brain lysates from $Dvl2^{+/+}$ and $Dvl2^{-/-}$ adults were used for Western blot analysis. Dvl2 protein was absent from $Dvl2^{-/-}$ brain lysates, and there was no compensatory increase of either Dvl1 or Dvl3 protein in mutant brains (Fig. 1D). PCR primers were developed that were effective in detecting both mutant and wild-type genotypes (Fig. 1E).

Perinatal lethality of 50% of $Dvl2^{-/-}$ mice

We examined mutant mice in inbred 129/SvEv or mixed 129/SvEv×NIH Black Swiss backgrounds and found that $Dvl2^{-/-}$ mice can survive to adulthood and are fertile, but they were born in reduced numbers from heterozygous crosses. Of 352 offspring at weaning, there were 130 $Dvl2^{+/+}$, 180 $Dvl2^{+/-}$ and only 42 $Dvl2^{-/-}$ mice, a reduction of more than 50% of expected numbers. However, at 18.5 dpc, $Dvl2^{+/+}$, $Dvl2^{+/-}$ and

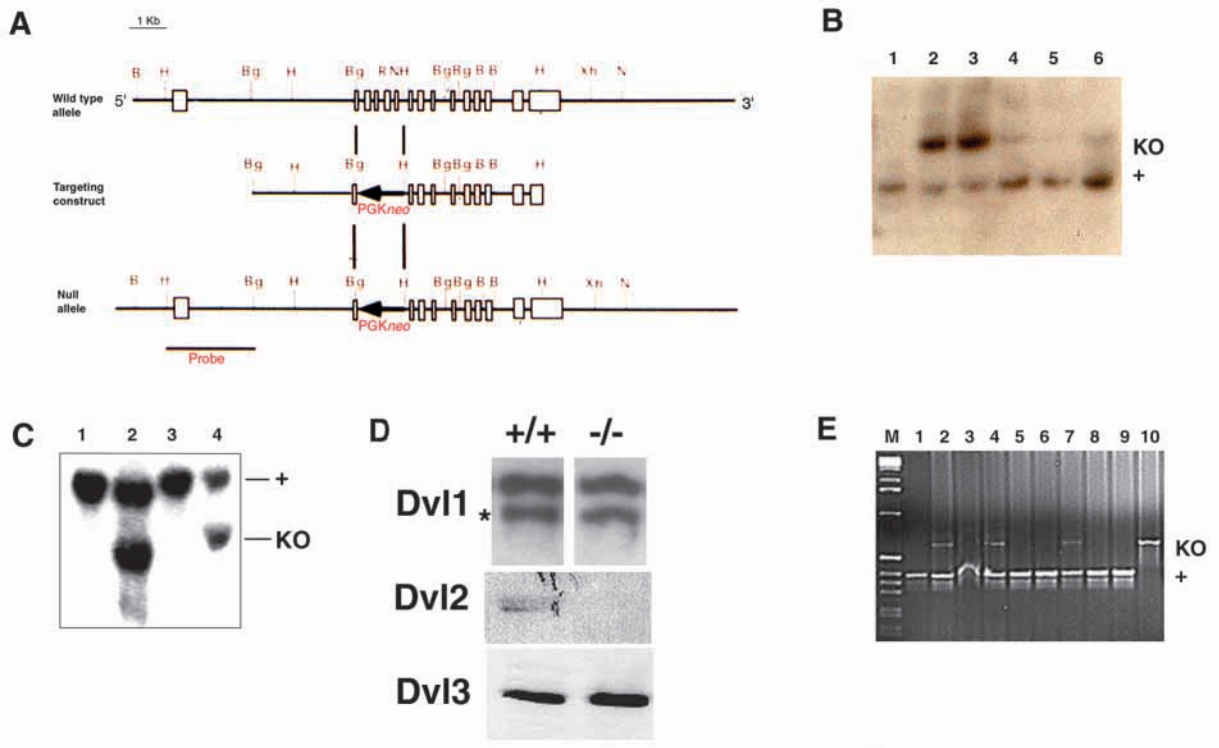

Fig. 1. Targeted inactivation of the *Dvl2* gene. (A) Diagrammatic representation of the wild-type *Dvl2* allele (top), the construct used for generating a null allele (middle) and the inactivated gene after homologous recombination (bottom). A PGKneo cassette was inserted in the opposite orientation relative to the start of *Dvl2* transcription in exon 2 and exons 3-6 were removed. (B) Southern blot analysis of genomic DNA from targeted (lanes 2-6) and wild-type (lane 1) embryonic stem cell clones digested with *Bam*HI/*Eco*RI and using the indicated 5′ flanking probe. The targeted band was approximately 3 kb larger because of the loss of the *Eco*RI site in exon 5. The positions of the targeted loci (KO) and the wild-type loci (+) are shown. (C) Southern blot analysis. Genomic tail DNA was digested with *Bam*HI and detected with the 5′ probe. The targeted allele was now smaller because a *Bam*HI site is included in the PGKneo cassette. (D) Immunoblot analysis. Brain lysates from $Dvl2^{+/+}$ and $Dvl2^{-/-}$ adults were used for western blot analysis, using C-terminal antibodies to Dvl1 (polyclonal), Dvl2 (monoclonal) and Dvl3 (monoclonal). No Dvl2 was detected in the $Dvl2^{-/-}$ samples. Dvl1 and Dvl3 protein levels were similar in both genotypes. Asterisk indicates Dvl1-specific band, identified by its absence in *Dvl1* mutant mice (data not shown). There is a higher molecular weight contaminant band used to assess loading. (E) PCR genotyping of genomic tail DNA. Upon amplification wild-type and knockout loci generate 391 bp and a 600 bp fragments, respectively. Lanes 1, 3, 5, 6, 8 and 9 are wild type; lanes 2, 4 and 7 are $Dvl2^{+/-}$; and lane 10 is a $Dvl2^{-/-}$ mouse.

Table 1. Genotype and sex ratios of adult offspring of *Dvl2* heterozygous crosses

	Dvl2$^{+/+}$		*Dvl2*$^{+/-}$		*Dvl2*$^{-/-}$	
	Male	Female	Male	Female	Male	Female
129 SvEv	10	9	29	30	2	13
	19		59		15	
Mix 129 SvEv/NIH Black Swiss	10	10	14	11	1	6
	20		25		7	
Combined	20	19	43	41	3	19
	39		84		22	

Dvl2$^{-/-}$ embryos were recovered in the expected mendelian ratios, suggesting that death occurred in the perinatal period. This was confirmed by directly observing litters at birth, where some newborn *Dvl2*$^{-/-}$ pups failed to thrive. Such pups appeared to have difficulty breathing, were often cyanotic, did not feed and displayed reduced mobility. These pups died within 24 hours. The perinatal lethality seemed to be unaffected by genetic influences caused by mouse strain modifiers as the survival percentages for *Dvl2*$^{-/-}$ mice were identical for both the mixed (16 observed out of 31 expected, n=125) and inbred strains (six observed out of 13 expected, n=51). Surprisingly, surviving *Dvl2*$^{-/-}$ mutants were predominantly female in either strain background (Table 1), suggesting an interaction between genotype and sex.

Dvl2$^{-/-}$ mice that survived beyond 24 hours grew normally into adulthood (2+ years) but ~25% (n=17) of the surviving mutant mice had kinked tails. A percentage of surviving *Dvl2* mutants also exhibited scoliosis and in rare instances displayed vestigial tail (n=3). This phenotype is very similar to the haploinsufficiency phenotypes seen in *Wnt3A* and *T* (brachyury) mutants (Yamaguchi et al., 1999). Embryo analysis in early gestation at 9.5 dpc revealed that 2-3% of *Dvl2*$^{-/-}$ embryos had incomplete thoracic neural tube defects (spina bifida) and exencephaly (see below). Serial sections of adult *Dvl2*$^{-/-}$ tissues showed no other morphological abnormalities (data not shown). Unlike the *Dvl1*$^{-/-}$ mice, *Dvl2*$^{-/-}$ homozygous mice displayed no abnormalities in social interaction or sensorimotor gating (data not shown).

Dvl2$^{-/-}$ lethality is due to cardiac anomalies

Dvl2$^{-/-}$ newborns had no abnormalities of the palate, trachea or lungs (data not shown). We next examined the hearts of 13, 18 and 20 dpc. *Dvl2*$^{-/-}$ animals obtained from *Dvl2*$^{+/-}$ crosses. Sixty-eight mice (16 *Dvl2*$^{+/+}$, 36 *Dvl2*$^{+/-}$ and 16 *Dvl2*$^{-/-}$ mice) were examined for cardiovascular defects. Eight *Dvl2*$^{-/-}$ (50%) of the mutant mice displayed cardiovascular abnormalities (Table 2). An additional embryo displayed a cardiac abnormality but was not included in Table 2 as genotype information for remaining littermates could not be determined because of a technical error. Eight *Dvl2*$^{-/-}$ embryos had structurally normal hearts, similar to the wild type (Fig. 2A,B). Double outlet right ventricle (DORV) was the most common defect and the placement of the aorta varied. Six mutant embryos had DORV in conjunction with ventricular septal defects (Fig. 2C,D, Fig. 3B). In one case of DORV the aorta emerged parallel to the pulmonary valve where the orientation of both great vessels were inverted and arose from the right ventricle (Fig. 2C,D). In fact, this was the most frequent manner in which DORV presented. One mutant had transposition of the great arteries (TGA). In addition, two of the mutant embryos had persistent or common truncus arteriosis (TA), a condition in which the outflow tract fails to divide into an aorta and pulmonary artery (Fig. 2E,F). These defects were clearly seen in serial sections of abnormal *Dvl2*$^{-/-}$ hearts (Fig. 3). TGA was evident in one heart (Fig. 3C) where the aorta emerged from the right ventricle. The severity of these defects would be sufficient to account for the perinatal lethality of *Dvl2*$^{-/-}$ mice. None of the *Dvl2*$^{+/-}$ or *Dvl2*$^{+/+}$ mice examined displayed any conotruncal abnormalities or other heart defects.

Table 2. Cardiovascular defects in *Dvl2*$^{-/-}$ and *Dvl1*$^{-/-}$;*Dvl2*$^{-/-}$ embryos

Abnormality	Wild type	*Dvl2*$^{+/-}$	*Dvl2*$^{-/-}$	*Dvl1*$^{-/-}$;*Dvl2*$^{-/-}$
Double outlet right ventricle	0	0	6	1
Transposition of the great arteries	0	0	1	1
Persistent truncus arterioisis	0	0	1	1
Normal	16/16	36/36	8/16	5/8*

*Two embryos had body wall defects but normal cardiac development.

In separate matings, *Dvl1*$^{-/-}$;*Dvl2*$^{-/-}$ embryos were examined for cardiac defects, to see if there was evidence for redundancy between *Dvl1* and *Dvl2* in conotruncal development. Of eight double homozygous embryos examined between 14.5 and 18.5 dpc, three displayed conotruncal defects (Table 2), including DORV, TGA and PTA. These results are consistent with a primary role for *Dvl2* in cardiac outflow tract development, and strongly suggest that *Dvl1* and *Dvl2* have non-redundant roles in heart morphogenesis.

Perturbation of cardiac neural crest expression in *Dvl2*$^{-/-}$ mice

The defects observed in the morphology of the great vessels in *Dvl2*$^{-/-}$ mice (DORV, TGA and PTA) are congenital heart defects that occur in embryogenesis due to abnormalities in outflow tract septation (Chien, 2000; Srivastava and Olson, 2000). Proper formation of the cardiac great vessels involves an early looping event occurring between 8.5-9.0 dpc followed by rotation of the developing conotruncal arteries. Between 11.5 and 12 dpc the developing conotruncus first rotates, followed by the development and fusion of the conotruncal cushions. As the endocardial cushions grow and migrate they develop chirality along the outflow tract. In the final step, the cushions fuse to form the aorticopulmonary septum. Cardiac neural crest cells are believed to migrate into the truncal cushions as they form and contribute to septation.

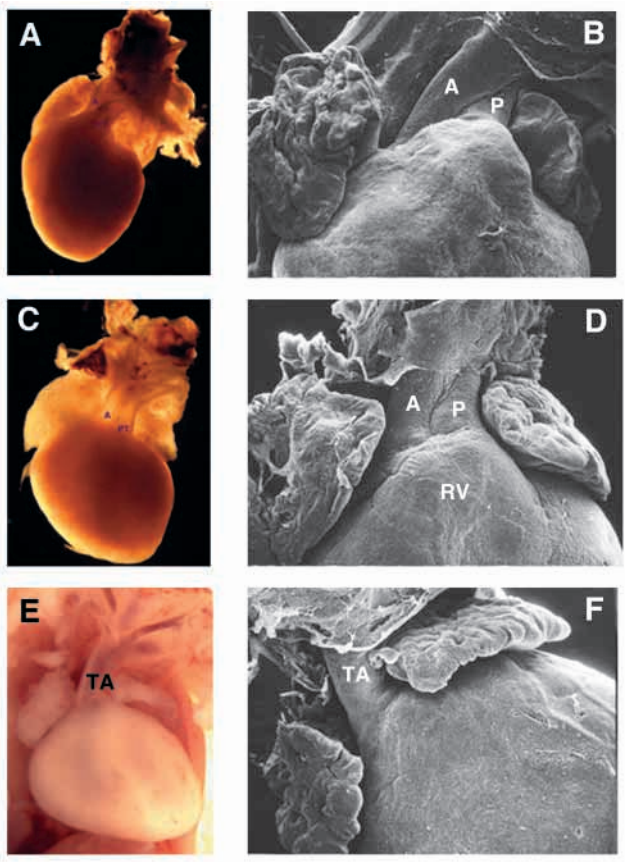

Fig. 2. Cardiovascular abnormalities in *Dvl2*$^{-/-}$ embryos. Frontal views of *Dvl2*$^{+/+}$ (A,B) and *Dvl2*$^{-/-}$ (C-F) hearts at 18.5 dpc. (A,C,E) Light microscope photograph; and (B,D,F) scanning electron microscopy (SEM) of identical hearts shown in left panel. (A,B) Normal heart outflow tract septation in which the pulmonary (PT) trunk arises from the right ventricle (RV) and the aorta (A) from the left ventricle (LV). The pulmonary trunk was located posteriorly and to the right rear of the aorta. The heart was rotated so that the right atrium was in the foreground, making the right atrium appear larger than the left atrium. The right atrium was visibly connected to the right ventricle. (C,D) In the most common defect observed in the *Dvl2*$^{-/-}$ mutants, both great vessels emerged from the right ventricle (DORV). The aorta was located to the left of and juxtaposed next to the pulmonary trunk. (E,F) A second defect observed in the *Dvl2*$^{-/-}$ hearts was the lack of two distinct outflow tract vessels. Instead a singular conotruncus emerged from the ventricle (PTA). No interventricular septum was visible. The ventricular surface was smooth and the irregularly shaped chamber was enlarged.

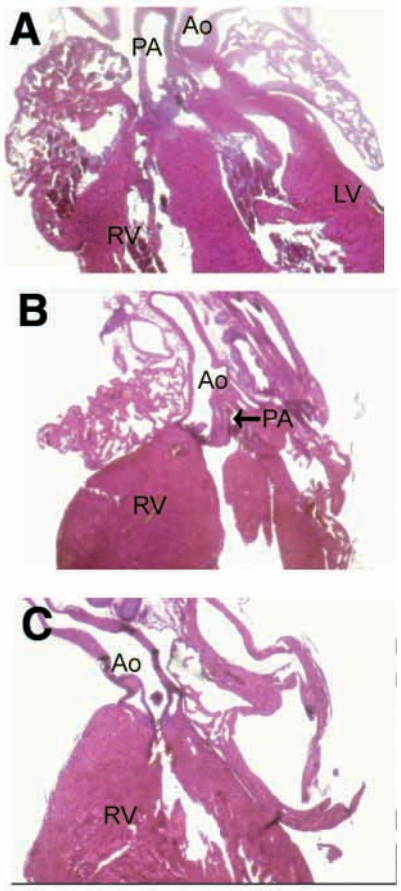

Fig. 3. Histological sections of *Dvl2*$^{+/-}$ and *Dvl2*$^{-/-}$ 18.5 dpc embryos stained with Hematoxylin and Eosin. (A) In the wild type, the right and left ventricle is divided by a membranous septum. (B) DORV and (C) transposition of the great arteries (TGA) in *Dvl2*$^{-/-}$ mutant. In B, the arrow indicates the pulmonary artery. Ao, aorta; PA, pulmonary artery; RV, right ventricle; LV, left ventricle.

Neural crest ablation studies have identified a subpopulation of neural crest cells at the level of the fourth and sixth aortic arch that affects proper septation termed the cardiac neural crest (Kirby et al., 1983; Creazzo et al., 1998; Kirby and Waldo, 1995).

Therefore, markers for early cardiac neural crest were employed, such as *Pitx2* and plexin A2. *Pitx2* is co-expressed with *Pax3*, connexin 43 and the endothelin receptor A in the cardiac neural crest, and *Pitx2* mutant mice display similar outflow tract defects as *Dvl2* (Kioussi et al., 2002). We used a *Pitx2* probe for whole mount analysis at 10.5 dpc In wild-type embryos, Pitx2 is normally expressed in a number of tissues, including the fourth branchial arch and migrating cardiac neural crest (Fig. 4A,C,E). *Dvl2*$^{-/-}$ embryos (Fig. 4B,D,F) and *Dvl1/2* double mutants (data not shown) had nearly undetectable levels of *Pitx2* in the branchial arches and in neural crest cells migrating to the cardiac outflow tract (Fig. 4B), as well as in the outflow tract (Fig. 4D,F). These results suggest that the outflow tract defects seen in *Dvl2*$^{-/-}$ mutant embryos are associated with cardiac neural crest defects. Subsequently, the expression of the cardiac neural crest marker *Plexin A2* (Brown et al., 2001) was examined. Plexin A2 expression was greatly reduced in hearts from *Dvl2*$^{-/-}$ (Fig. 4H) mutant embryos compared with wild-type hearts (Fig. 4G), further supporting the notion that the conotruncal defects displayed by *Dvl2*$^{-/-}$ mutants result from neural crest abnormalities.

Skeletal defects in *Dvl2*$^{-/-}$ and *Dvl1/2* double mutant mice

As part of our phenotypic analysis, we examined bone and cartilage development using Alizarin Red and Alcian Blue staining in 18 *Dvl2*$^{-/-}$ newborns. Nearly all (90%) of the *Dvl2* mutant mice displayed mild abnormalities of the vertebral

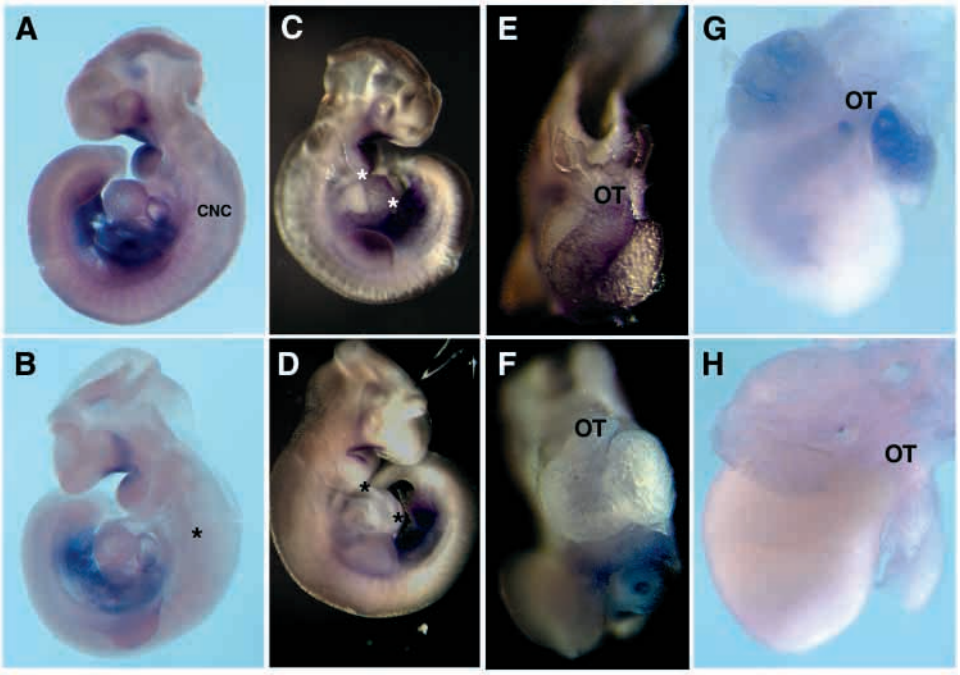

Fig. 4. In situ analysis using *Pitx2* and *PlexinA2* as markers of cardiac neural crest. (A-F) *Pitx2* was used as a probe on wild-type (A,C,E) and *Dvl2*$^{-/-}$ (B,D,F) embryos at 10.5 dpc. (A,B) The left side views reveal signal in the branchial arches and migrating cardiac neural crest of wild-type (CNC in A) but not *Dvl2*$^{-/-}$ embryos (asterisk in B). (C,D) The right sided views reveal signal in the outflow tract (outlined by two asterisks) of wild-type (C), but not *Dvl2*$^{-/-}$ embryos (D). (E,F) Embryos in C and D were dissected to reveal staining in the cardiac outflow tract (OT) of wild-type (E) but not *Dvl2*$^{-/-}$ mutant (F) embryos. (G,H) Plexin A2 was used as a probe for migrating neural crest cells in the outflow tract (OT) of hearts, which were present in wild-type (G) but not *Dvl2*$^{-/-}$ hearts (H) at 10.5 dpc.

bodies and ribs (Fig. 5, Table 3). Most defects were localized dorsally in the vertebral ribs and vertebral bodies (Fig. 5A-E). Many of the abnormal thoracic vertebrae were disorganized (Fig. 5A) and fusion of the ribs near the tubercle was evident (Fig. 5B). We determined whether the normal rib number was altered in any of the mutant mice. In all but one case we found that in the presence of either forked or fused ribs the total rib number on both the left and right sides was 13. These findings suggest that the normal number of ribs was specified, but segmentation did not occur properly. *Dvl1/2* double homozygotes had more severe skeletal malformations of the type seen in *Dvl2*$^{-/-}$ mice (Fig. 5F). For example, a 14.5 dpc. double mutant embryo demonstrated numerous collapsed vertebrae and extensive fusion of the ribs along the vertebral column. These defects were not observed in *Dvl1*$^{-/-}$ mice (Lijam et al., 1997), suggesting that functional redundancy restricted this phenotype in either *Dvl1*$^{-/-}$ or *Dvl2*$^{-/-}$ single mutants.

A sternal defect was detected in one newborn mouse, and affected the sixth sternebra and the xiphoid process (Fig. 5H). A completely split or perforated xiphoid process was evident. Seven ribs are attached to the sternum but no malformations were detected in any of the seven sternal ribs. Overall, these data demonstrate that *Dvl2* is essential for proper formation of ribs, vertebral bodies and sternum.

Somite analysis using paraxial mesodermal markers

Somites originate as cells that pinch off from the presomitic mesoderm. As the somite condenses, it develops into a disorganized ball of cells internally surrounded by a layer of columnar epithelial cells. The basolateral wall of the epithelial cell undergoes an epithelial-to-mesenchymal transition that results in the formation of sclerotome ventrally and dermomyotome dorsally. The sclerotome and dermomyotome collectively give rise to the cartilage, bone, muscle and connective tissue (Keynes and Stern, 1988; Huang et al., 2000). In addition, anterior and posterior domains exist within the sclerotome as demonstrated with mesodermal probes that identify these distinct cell populations. To investigate somite differentiation in the *Dvl2* single and *Dvl1/2* double mutants, we performed whole-mount in situ hybridization using a variety of somite markers.

No differences were found between wild-type and *Dvl2*$^{-/-}$ mutants using several markers, including the caudal somite markers *Uncx4.1*, delta 1 and lunatic fringe, as well as the rostral marker delta 3 (data not shown). To determine whether the axial defects that affect rib fusion could be due to abnormalities that precede somite division into caudal and rostral halves, we used probes that identify the presomitic mesoderm. There were no alterations in the coordinated expression of *Notch1* or *Notch2* in wild-type and *Dvl2*$^{-/-}$ mutants (Fig. 6C-F). However, myogenin, a myotomal marker, was occasionally attached between two somites of *Dvl2* mutants as a bridge (Fig. 6A,B), suggesting that abnormal, incomplete segmentation could be the cause of the somite defects seen in these mutants.

As *Dvl1/2* double mutants display rib and vertebral defects of the same type seen in *Dvl2*$^{-/-}$ mice, but of more severe extent and at higher frequency, we examined the expression pattern of somite markers in the double mutants, hoping to increase the chance that relevant abnormalities in marker expression

Table 3. Skeletal defects in *Dvl2*$^{-/-}$ 18.5 dpc fetuses

Phenotype	Number affected
Forked vertebral rib	9/18
Fused vertebral rib	9/18
Other rib anomaly	1/18
Left or right side affected	9/18
Both rib sides affected	6/18
Abnormal vertebral bodies	16/18
Sternal rib defect (xiphoid process)	1/18
No abnormality observed	2/18

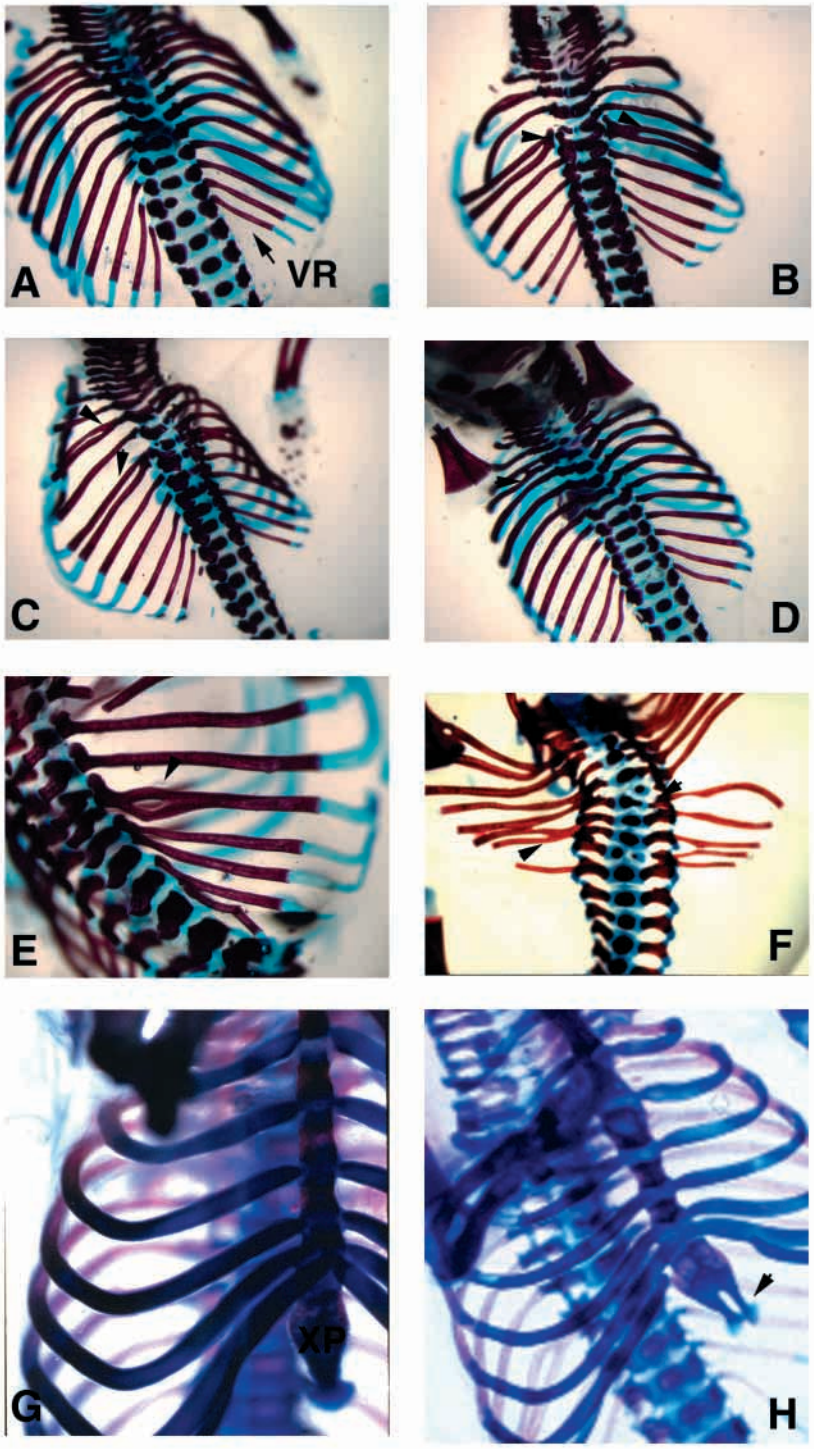

Fig. 5. *Dvl2*$^{-/-}$ mutant mice show variable rib defects. At 18.5 dpc, embryos were stained with Alizarin Red (bone) and Alcian Blue (cartilage). (A) Thirteen distinct ribs are attached to a complementary vertebral body, but there is a hemivertebrae at the 12th rib. Sternal ribs are seen in the background, while vertebral ribs are in the foreground. Vertebral ribs occasionally show an inappropriate fusion at the proximal rib site (arrowheads, B) or at slightly more distal regions of the rib (arrowheads in C). An abnormal ossification bridge links two neighboring vertebral ribs in some mutants (arrowhead in D). (E) Vertebral rib from *Dvl2*$^{-/-}$ E18.5 embryo showing a bowed perforation in the proximal vertebral rib. (F) *Dvl1*$^{-/-}$ *Dvl2*$^{-/-}$ double mutant showing irregular rib fusion and splitting of ribs along the vertebral column (arrowheads). Abnormalities in the cervical and thoracic vertebrae are evident. The sternum has been cut to better visualize the rib defects. Frontal view of sternum from a wild-type (G) and *Dvl2*$^{-/-}$ mutant (H) 18.5 dpc embryo. During development the ribs move ventromedially and fuse inhibiting bone formation at the contact sites and forming ossification centers around these sites termed sternbrae. Defects detected in sternbrae 6 and the xiphoid process (XP) of *Dvl2*$^{-/-}$ mutants include bifurcation (arrowhead, H) as well as perforations.

would be observed. Similar to the results for myogenin in *Dvl2*$^{-/-}$ mice, *Uncx4.1* was detected in a fused band between adjacent somites, indicating incomplete segmentation of these two somites (Fig. 6I,J) in the *Dvl1/Dvl2* double mutant embryo. The caudal probe delta 1 was expressed throughout the appropriate regions of the somite, but the spacing was irregular in the double mutant (Fig. 6K,L). In both of these cases, the abnormal somites appear to be split, consistent with the normal ultimate rib and vertebral numbers of the *Dvl2* and *Dvl1/2* mutants. Lunatic fringe transcripts were present in the forebrain, placodes, neural tube and dermomyotome of the wild-type embryo (Fig. 6G). Overall, this pattern was repeated for the *Dvl1/2* mutant but expression in the dermomyotome was markedly depressed (inset Fig. 6H). No differences were found in *Dvl1/2* double mutants using delta 3. Thus, minor abnormalities were evident in somite precursors of *Dvl2* mutants, which were more severe in the *Dvl1/2* double mutant. These defects appear to be due to mild abnormalities in somite segmentation.

Neural tube defects in *Dvl2*$^{-/-}$ and *Dvl1/2* double mutant mice

Approximately 2-3% of *Dvl2* homozygotes have incomplete thoracic neural tube defects (Fig. 7B), often associated with exencephaly, compared with normal neural tube closure in wild-type embryos (Fig. 7A). Although the penetrance was low, we reasoned that there may be functional redundancy among the Dvl genes because of their overlapping patterns of expression and structural similarity. To test for functional redundancy, *Dvl1*$^{+/-}$;*Dvl2*$^{+/-}$ double heterozygous crosses and *Dvl1*$^{-/-}$;*Dvl2*$^{+/-}$ crosses were performed. Litters were genotyped at weaning. No *Dvl1*$^{-/-}$;*Dvl2*$^{-/-}$ mice were identified (20 expected, none observed, n=230). Embryos were dissected at various times from these crosses. Surprisingly, we found that *Dvl1*$^{-/-}$;*Dvl2*$^{-/-}$ embryos (Fig. 7C) displayed completely open spinal neural tubes and exencephaly (cranio-rachischisis). The neural tube closure defects resulted in the development of the brain outside of the cranium, and the spinal cord was completely open to the base of the tail. The face was fused, as

was the tail, suggesting that some regions of the neural tube closed normally. At 9.5-10.5 dpc, the neural tubes of wild-type embryos were completely closed in the midbrain, hindbrain and thoracic region (Fig. 7D), while the neural tubes of *Dvl1/Dvl2* double mutants were completely open from the midbrain to the tail (Fig. 7E). Of 380 embryos dissected between 8.5 and 10.5 dpc from both $Dvl1^{+/-};Dvl2^{+/-}$ double heterozygous crosses and $Dvl1^{-/-};Dvl2^{+/-}$ crosses, 40 $Dvl1^{-/-};Dvl2^{-/-}$ double homozygotes were observed (45 expected). Of these, 31 had open unfused neural tubes, one had an open neural tube with fused epidermal ectoderm, six had partially open neural tubes and two appeared normal.

There were clear defects in the developing spinal cord and brain resulting from closure defects. In spite of such defects, there appeared to be recognizable regional differentiation of forebrain, midbrain and hindbrain regions, even though there was marked disorganization secondary to exencephaly (Fig. 7F,G). Similarly, the dorsal and ventral regions of the mutant open spinal cord were recognizable (Fig. 7H,I).

Thus, *Dvl2* is essential for neural tube closure in mice, and there are overlapping functions between *Dvl1* and *Dvl2* in neurulation.

DISCUSSION

We have generated mice carrying null mutations in *Dvl2* and have found that 50% of *Dvl2* null mutants display perinatal lethality because of defects in cardiac morphogenesis. Specifically, outflow tract septation defects were observed in approximately 50% of $Dvl2^{-/-}$ mice analyzed in late gestation, including DORV with VSD, PTA and TGA. These cardiac defects are incompatible with life and would account for the perinatal lethality of *Dvl2* mutants. These findings demonstrate

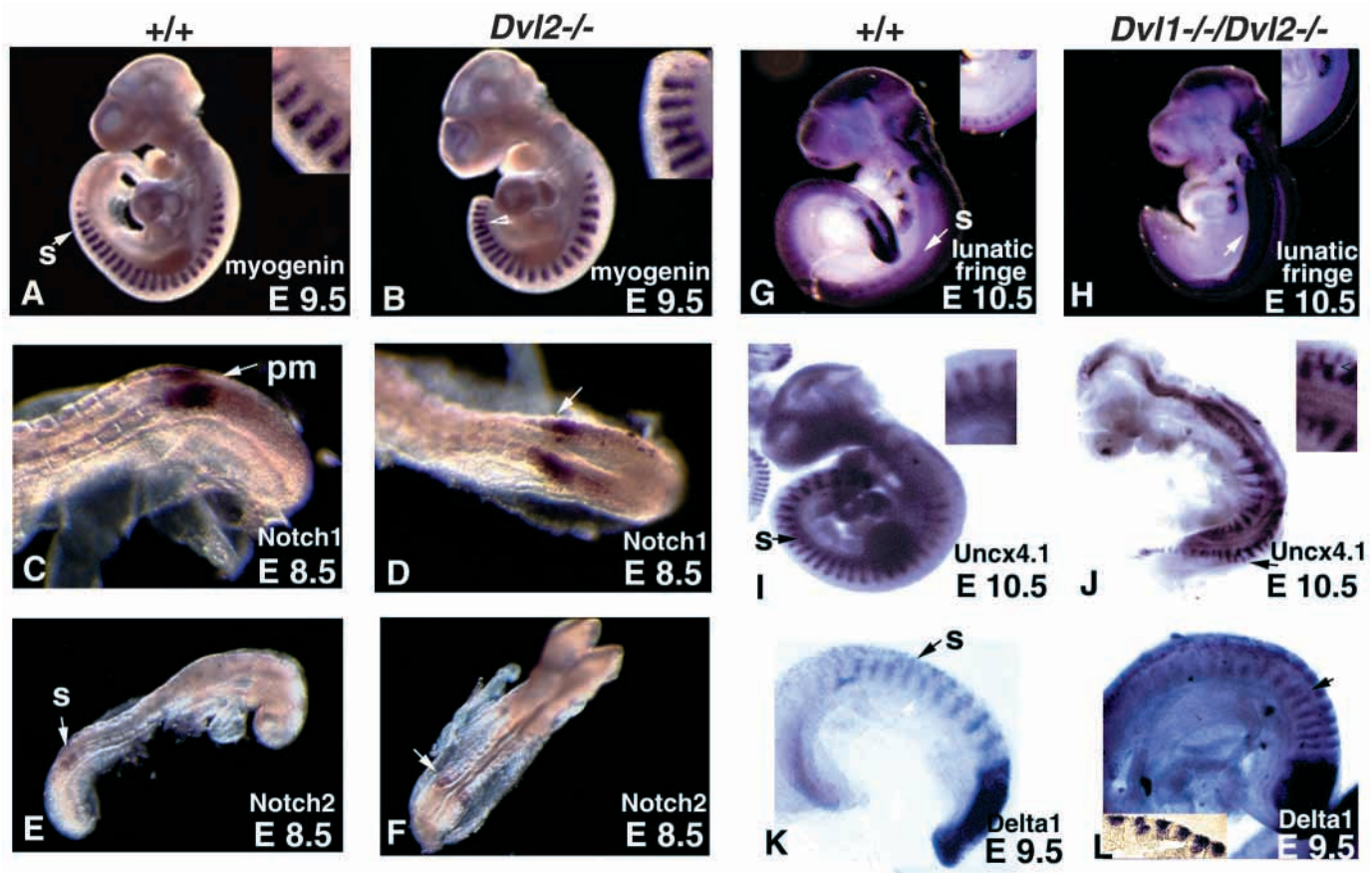

Fig. 6. Expression of mesodermal markers in wild-type, $Dvl2^{-/-}$ and $Dvl1^{-/-}$ $Dvl2^{-/-}$ embryos. Whole-mount in situ hybridization was carried out on E8.5, E9.5 and E10.5 embryos. Labeling with myogenin, a myotomal marker, revealed abnormal segmentation into somites (S) of $Dvl2^{-/-}$ embryos (B). The regular metameric pattern seen in wild-type embryos (A) was maintained in mutant embryos (B) except for a distinct band of expression connecting two somites (B, arrowhead and inset). (C-F) Coordinated segmentation was normal in $Dvl2^{-/-}$ mutants. *Notch1* was properly expressed in the presomitic mesoderm (pm, arrow) of the wild-type (C) and of the $Dvl2^{-/-}$ mutant embryo (D). Two pairs of newly forming somites were seen on either side of the neural tube (S and arrow in E,F) in wild-type (E) and $Dvl2^{-/-}$ (F) embryos using *Notch2*, a presomitic marker. Wild-type (+/+, G,I,K) and *Dvl1/Dvl2* double homozygous embryos ($Dvl1^{-/-}$ $Dvl2^{-/-}$, H,J,L). Expression of lunatic fringe was detected in neural tube, tail mesoderm, rhombomeres and sclerotome of wild-type and $Dvl1^{-/-}$ $Dvl2^{-/-}$ double knockouts but expression in the sclerotome was decreased in the mutant embryo (inset H). (I,J) The posterior sclerotomal marker *Uncx4.1* reveals normal expression in the somites of wild-type embryos but this pattern was disrupted in caudal somites of the $Dvl1^{-/-}$ $Dvl2^{-/-}$ embryo. In the mutant embryo (J) the somite signal was not as distinct as that of the normal embryo (I) and two stripes of *Uncx4.1* expression were fused in the mutant (inset J). (K,L) Delta 1 was normally expressed in the caudal somite of wild-type (white arrowhead in K) and mutant embryos but abnormal expression was detected in some somites of the $Dvl1^{-/-}$ $Dvl2^{-/-}$ embryo (arrows). An additional patch of expression was detected in a sagittal section of the mutant somite (inset L).

a novel role for a dishevelled gene in cardiac development and specifically identify *Dvl2* as a key mediator in conotruncal development. There was no evidence for redundancy between *Dvl1* and *Dvl2*, as the penetrance of cardiac defects was similar in *Dvl2* and *Dvl1/2* mutants. In addition, almost all (90%) of the *Dvl2* homozygous newborn null mice displayed abnormalities in patterning of the axial skeleton in which the sternal ribs and the vertebrae were affected. These defects appeared to be due to perturbations in the segmentation of the somites, implicating *Dvl2* in the control of somitogenesis. These segmentation defects were even more severe in *Dvl1/2* double mutants, suggesting a dose dependence of Dvl gene function in somite formation. Finally, 2-3% of *Dvl2* null mice exhibited spina bifida. Similar to somite segmentation, defects in neural tube development were even more pronounced in mice deficient for both *Dvl1* and *Dvl2*. *Dvl1*$^{-/-}$;*Dvl2*$^{-/-}$ mice display a completely open neural tube with craniorachischisis indicating that the increase in severity of the neural tube phenotype is also Dvl-dose dependent. These results demonstrate that although there is significant functional redundancy between *Dvl1* and *Dvl2* in somite development and neural tube closure, a somewhat unique role in cardiac outflow tract patterning can be assigned to *Dvl2*.

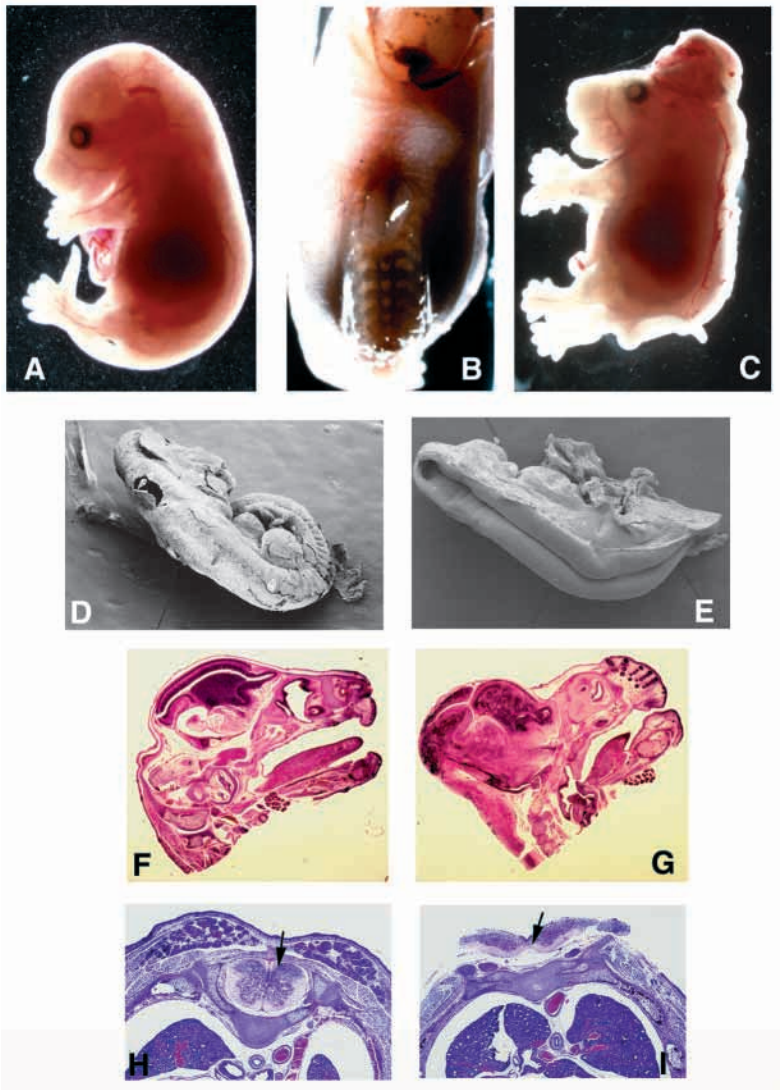

Fig. 7. Neural tube defects in *Dvl2*$^{-/-}$ and *Dvl1*$^{-/-}$;*Dvl2*$^{-/-}$ mice. (A) Lateral view of wild-type 14.5 dpc embryo. (B) Example of spinal bifida and exencephaly seen at low penetrance (2-3%) in an 14.5 dpc *Dvl2*$^{-/-}$ embryo. (C) Craniorachisis was evident in *Dvl1/Dvl2* double mutant littermate The tail was frequently tightly curled. All other major body structures were normal, including the limbs and face. (D) The neural tube was completely closed in wild-type embryos at 10.5 dpc. (E) SEM studies at 9.5 dpc revealed a severe open neural tube that extends from the midbrain-hindbrain junction to the tail. The posterior region of the *Dvl1/Dvl2* double mutant just rear of the hindlimb bud was truncated as there was the loss of a properly formed tail and rostral somites. Sagittal sections through 14.5 dpc *Dvl1*$^{-/-}$;*Dvl2*$^{-/-}$ embryonic head (G) indicated major brain regions were present but disorganized in the mutant embryos when compared with wild type (F). (H,I) Transverse sections through the thoracic cavity. The spinal cord of *Dvl1/Dvl2* double mutant embryos (I) was open but recognizable with a well differentiated floor plate (arrow), compared with wild type (H).

Mice with targeted inactivation of the *Dvl1* gene have been previously described (Lijam et al., 1997). These mice were found to exhibit alterations in sensorimotor gating and social interaction. Surprisingly *Dvl2* does not seem to play a similar role in the regulation of social behavior or sensorimotor gating, as no abnormalities in these processes were observed. These observations suggest a unique function for *Dvl1* in social behavior and sensorimotor gating.

The heart phenotype manifested by the loss of *Dvl2* was specific to the outflow tract. Proper alignment and development of the aorticopulmonary septum involves migration and fusion of the endocardial cushions, as well as a correct pivoting event along the axis that forms the AV canals. Genes that affect early cardiac looping such as *Nkx2.5*, *Mef2c*, as well as the bHLH proteins *Hand1* and *Hand2* have been identified (Olson and Srivastava, 1996; Thomas et al., 1998; Srivastava et al., 1995; Lyons et al., 1995; Lin et al., 1997; Bruneau et al., 2000). Improper cardiac looping can lead to outflow tract defects and tetratolgy of Fallot based on studies in the mouse (Srivastava, 2000; Creazzo et al., 1998; Olson and Srivastava, 1996).

In the case of *Dvl2* mutants, a defect in cardiac neural crest appears to be responsible for the observed outflow tract defects. Cardiac neural crest cells are essential for normal development of the outflow tract. These cells originate from the caudal hindbrain and migrate into the caudal pharyngeal arches (third, fourth and sixth). A subset of these cells continues to migrate into the cardiac outflow tract where it will organize the aorticopulmonary septum. If cardiac neural crest cells are removed prior to migration, several predictable outflow tract phenotypes are observed after development of the heart and great arteries is complete, including DORV, TGA and PTA (Kirby et al., 1983; Creazzo et al., 1998) (reviewed by Kirby and Waldo, 1995; Chien, 2000). *Pitx2* is co-expressed with *Pax3* in the cardiac neural crest, and *Pitx2* mutant mice display similar outflow tract defects as *Dvl2* (Kioussi et al., 2002).

Plexin A2 has recently been identified as a marker for cardiac neural crest that is expressed at later times in development (Brown et al., 2001). Therefore, we examined the expression of *Pitx2* and plexin A2 in *Dvl2* and *Dvl1/2* mutant mice. Expression of these markers along the migrating cardiac neural crest were impaired in Dvl mutant mice, implicating the neural crest in the outflow tract defects displayed by *Dvl2*$^{-/-}$ mice.

We recently found that *Dvl2* and *Pitx2* were part of a common pathway regulating proliferation in specific tissues (Kioussi et al., 2002). We found that *Dvl2* and *Pitx2* genetically interact to produce cardiac outflow tract abnormalities. We further demonstrated that Pitx factors can exert essential roles in cardiac neural crest cell development based on the β-catenin-dependent transcriptional induction of *Pitx2*. Pitx2, in turn, acts upstream of genes required for the cell proliferation program, including cyclin D1 and cyclin D2. Components of this Wnt/Dvl/β-catenin→Pitx2 pathway are required, in a dose-dependent fashion, for physiological proliferation of specific cells within the cardiac outflow tract, in particular the cardiac neural crest, and pituitary gland. These findings strongly support our interpretation that the primary outflow tract defect in *Dvl2* mutant mice is in the cardiac neural crest. In addition, they suggest that Dvl2 and Pitx2, among other proteins, could be novel components of a multigenic origin of cardiac outflow tract defects that occur in the human population. As cardiac outflow tract abnormalities account for ~30% of all cardiovascular malformations in humans (Chien, 2000; Srivastava and Olson, 2000), this pathway could be important for human conotruncal defects as well.

These findings support a role for the Wnt pathway in cardiac morphogenesis through the control of cardiac neural crest development. There is some earlier evidence that the Wnt pathway plays an important role in cardiac morphogenesis, beginning with studies using antisense attenuation of *Wnt1* and *Wnt3a* expression in whole embryo cultures (Augustine et al., 1993). Recent reports demonstrate that Wnt inhibition induces cardiogenesis in *Xenopus* (Schneider and Mercola, 2001) and in chick (Marvin et al., 2001), but the role of Wnt signaling in mammalian systems was unclear. So far, no Wnt pathway mutants display cardiac defects. However, neural crest abnormalities do occur in the *Wnt1/Wnt3a* double mutant. In addition, using a floxed β-catenin allele and the Wnt1-Cre transgenic mouse that expresses Cre in the neural crest, we were able to delete β-catenin completely in the neural crest. These mice displayed similar conotruncal defects as the *Dvl2*$^{-/-}$ mice (Kioussi et al., 2002), consistent with a role for Dvl2 in the cardiac neural crest.

Downstream of *Dishevelled*, the *Notch* and *Wnt* pathways have both been implicated in somite formation and segmentation. Members of the *Notch* pathway are intimately involved in controlling somitogenesis (reviewed by Muskaitch et al., 1994; Artavanis-Tsakonas et al., 1999), including *Notch1* (Conlon et al., 1995), *Notch2*, delta 3 (Kusumi et al., 1998) and lunatic fringe (Evrad et al., 1998; Zhang et al., 1998). *Notch* is downstream of *Dsh* in *Drosophila* (Axelrod et al., 1996; Couso and Martinez Arias, 1994). *Notch1* and *Notch2* expression were normal in the somites of *Dvl2* mutants, indicating that development of the somites from presomitic mesoderm was unperturbed. However, somite segmentation was abnormal as defined by expression of the sclerotomal marker *Uncx4.1*. These expression alterations were not identical to the severe defects displayed by Notch pathway mutants. Instead, rather subtle but distinct alterations in somite boundaries were evident as detected by the delta 1 and lunatic fringe. *Wnt3a* is also involved in paraxial mesoderm differentiation. *Wnt3a* mutants exhibit posterior truncation and lack a significant number of posterior somites (Takada et al., 1994). The somite defects in the *Dvl2* mutant mice reflect mild defects in segmentation, rather than conversion of posterior to anterior fates, but a role for Dvl genes in posterior development cannot be completely ruled out.

Dvl2 is essential for normal neural tube closure, because a small number of embryos display thoracic spina bifica and exencephaly. Neural tube defects (NTDs) are a common class of birth defects in humans with an incidence that varies from 0.5-8 per 1000 live births (Elwood et al., 1992). Several factors are associated with NTDs, including genetic factors, teratogens and low levels of dietary folate. There is wide variation in the type and severity of NTDs in humans. Genetic epidemiology studies have suggested that NTDs have a multifactorial etiology with genetic predisposition because of many genes and a threshold beyond which environmental factors can trigger NTDs during crucial fetal periods. Several mouse mutants display NTDs. More than 50 loci have been identified, and many of the mutant alleles have been cloned (Juriloff and Harris, 1999). We have now identified *Dvl2* as an additional locus important for neural tube closure. In addition, there is functional redundancy between *Dvl1* and *Dvl2* in neural tube closure, as the double mutants display a completely open neural tube between the midbrain and tail, termed craniorachischisis.

Loop tail (*Lp*) is one other mouse mutant that displays cranio-rachischisis (Greene et al., 1998). The gene for *Lp* has been cloned (Kibor et al., 2001; Murdoch et al., 2001) and codes for a transmembrane protein loopin with a PDZ-binding domain. *Ltap* is related to the *Drosophila* gene *Van Gogh*, which is downstream of *frizzled* and *Dishevelled* in the planar cell polarity (PCP) pathway (Taylor et al., 1998; Wolff and Rubin, 1998). These finding suggest the intriguing possibility that mammalian *Dvls* and *Lp* are in a common PCP-like pathway mediating neural tube closure. In *Xenopus*, *Dishevelled* is an integral part of the PCP pathway that regulates gastrulation via convergent extension (Wallingford et al., 2000), and has also been implicated in neural tube closure in *Xenopus* (Wallingford and Harland, 2001; Wallingford et al., 2002). The *Dvl1/Dvl2* phenotype may be the result in defects of convergent extension mechanisms via the PCP pathway, suggesting that *Dvl1*, *Dvl2* and *Lp* are part of a common PCP pathway regulating neurulation in the mouse.

In summary, we have provided evidence that *Dvl2* is important for cardiac outflow tract development via the cardiac neural crest, somite segmentation and neural tube closure. These findings, together with previously published (Lijam et al., 1997) and unpublished results, demonstrate that *Dvl1* and *Dvl2* are partially redundant, but also have unique functions. Somite segmentation and neural tube closure appear to be mediated by overlapping redundant functions that are dependent on the dose of these two genes. By contrast, social interaction and sensorimotor gating defects are unique to *Dvl1* mutants, while cardiac defects appear to be unique to *Dvl2* mutants. The *Dvl1* and *Dvl2* mutant mice will be invaluable tools with which to continue to sort out the important pathways

regulated by *Dishevelled* genes to regulate complex behavior, cardiac outflow tract development and somite segmentation.

We are grateful to Ron Conlon, Randy Johnson, Tom Gridley and Chin Chiang who all provided probes for in situ analysis. We wish to thank Denise Larson, (NIH/NHGRI) Lisa Garrett, Theresa Hernandez (NIH/NHGRI Transgenic Core), Elaine Cheung (UCSD) and Kevin Nyguen (UCSD) for their technical assistance. We also wish to thank Charles Graham at the SIO Analytical Facility and Debbie Beiley (UCSD) for her continuous help in the preparation of this manuscript.

REFERENCES

Artavanis-Tsakonas, S., Rand, M. and Lake, R. J. (1999). Notch signaling: cell fate control and signal integration in development. *Science* **284**, 770-776.

Augustine, K., Liu, E. T. and Sadler, T. W. (1993). Antisense attenuation of Wnt1 and Wnt 3A expression in whole embryo culture reveals roles for these genes in craniofacial, spinal cord and cardiac morphogenesis. *Dev. Genet.* **14**, 500-520.

Axelrod, J., Matsuno, K., Artavanis-Tsakonas, S. and Perrimon, N. (1996). Interaction between wingless and notch signaling pathways mediated by dishevelled. *Science* **271**, 1826-1832.

Axelrod, J., Miller, J., Shulman, J., Moon, R. and Perrimon, N. (1998). Differential recruitment of Dishevelled provides signaling specificity in the planar cell polarity and wingless signaling pathways. *Genes Dev*. **12**, 2610-2622.

Bejsovec, A. and Arias, A. (1991). Roles of wingless in patterning the larval epidermis of Drosophila. *Development* **113**, 471-485.

Boutros, M., Parcio, N., Strutt, D. and Mlodzik, M. (1998). Dishevelled activates JNK and discriminates between JNK pathways in planar ploarity and wingless signaling. *Cell* **94**, 109-118.

Brown, C. B., Feiner, L., Lu, M.-M., Li, J., Ma, X., Webber, A. L., Jia, L., Raper, J. A. and Epstein, J. A. (2001). PlexinA2 and semaphorin signaling during cardiac neural crest development. *Development* **128**, 3071-3080.

Bruneau, B. G., Bao, Z. Z., Tanaka, M., Schott, J. J., Izumo, S., Cepko, C. L., Seidman, J. G. and Seidman, C. E. (2000). Cardiac exxpression of the ventricle-specific homeobox gene Irx4 is modulated by Nkx2.5 and dHAND. *Dev. Biol*. **217**, 266-277.

Cadigan, K. M. and Nusse, R. (1997). Wnt signaling: a common theme in animal development. *Genes Dev.* **11**, 3286-3305.

Chien, K. R. (2000). Genomic circuits and the integrative biology of cardiac diseases. *Nature* **407**, 227-232.

Conlon, R., Reaume, A. and Rossant, J. (1995). Notch1 is required for the coordinate segmentation of somites. *Development* **121**, 1533-1545.

Couso, J. and Martinez Arias, A. (1994). Notch is required for wingless signaling in the epidermis of Drosophila. *Cell* **79,** 259-272.

Creazzo, T., Godt, R., Leatherbury, L., Conway, S. and Kirby, M. (1998). Role of cardiac neural crest cells in cardiovascular development. *Annu. Rev. Physiol*. **60**, 267-286.

Deng, C., Wynshaw-Boris, A., Kuo, A., Zhou, F. and Leder, P. (1996). Fibroblast growth factor receptor-3 is a negative regulator of bone growth and development. *Cell* **84**, 911-921.

Elwood, J. M., Little, J. and Elwood, L. H. (1992). Epidemiology and control of neural tube defects. New York: Oxford University Press.

Evrad, Y., Lun, Y., Aulehia, A., Gan, L. and Johnson, R. (1998). Lunatic fringe is an essential mediator of somite segmentation and patterning. *Nature* **394**, 377-381.

Greene, N. D., Gerrello, D., van Stratten, H. W. and Copp, A. J. (1998). Abnormalities of floor plate, nototchord and somite differentiation in the *loop-tail* (*Lp*) mouse: a model of severe neural tube defects. *Mech. Dev.* **73**, 59 (1998).

Huang, R., Zhi, Q., Schmidt, C., Wilting, J., Brand-Serberi, B. and Christ, B. (2000). Sclerotomal origin of the ribs. *Development* **127**, 527-532.

Ikeya, M., Lee, S., Johnson, J., McMahon, A. and Takada, S. (1997). Wnt signaling required for expansion of neural crest and CNS progenitors. *Nature* **389**, 966-970.

Juriloff, D. M. and Harris, M. J. (1999). Mini-review: toward understanding mechanisms of genetic neural tube defects in mice. *Teratology* **60**, 292-305.

Keynes, R. and Stern, C. (1988). Mechanisms of vertebrate segmentation. *Development* **103**, 413-429.

Kibor, Z., Vogan, K. J., Groulx, N., Justice, M., Underhill, D. A. and Gros, P. (2001). *Ltap*, a mammalian homolog of *Drosophila Strabismus*/*Van Gogh*, is altered in the mouse neural tive mutant Loop-tail. *Nat. Genet.* **28**, 251-255.

Kioussi, C., Briata, P., Baek, S. H., Rose, D., Hamblet, N. S., Herman, T., Lin, C., Gleiberman, A., Wang, J., Brault, V., Ruiz-Lozano, P., Nguyen, H. D., Kemler, R., Glass, C. K., Wynshaw-Boris, A. and Rosenfeld, M. G. (2002). A Wnt/Dvl->Pitx pathway reveals molecular mechanisms for mediating cell type-specific proliferation during development. *Cell* (in press).

Kirby, M. L., Gale, T. F. and Stewart, D. E. (1983). Neural crest cells contribute to normal aorticopulmonary septation. *Science*, **220**, 1059-1061.

Kirby, M. L. and Waldo, K. L. (1995). Neural crest and cardiovascular patterning. *Circ. Res.* **77**, 211-215.

Kishida, S., Yamamoto, H., Hino, S., Ikeda., M. and Kikuchi, A. (1999). DIX domains of Dvl and axin are necessary for protein inbteractions and their ability to regulate beta-catenin. *Mol. Cell Biol*. **19**, 4414-4422.

Klingensmith, J., Nusse, R. and Perrimon, N. (1994). The *Drosophila* segment polarity gene *dishevelled* encodes a novel protein required for response to the *wingless* signal. *Genes Dev*. **8**, 118-130.

Klingensmith, J., Yang, Y., Axelrod, J. D., Beier, D. R., Perrimon, N. and Sussman, D. J. (1996). Conservation of dishevelled structure and function between flies and mice: isolation and characterization of *Dvl2*. *Mech. Dev.* **58**, 15-26.

Kusumi, K., Sun, E., Kerrerock, A., Bronson, R., Chi, D., Bulotsky, M., Spencer, J., Birren, B., Frankel, W. and Lander, E. (1998). The mouse pudgy mutation disrupts Delta homologue Dll3 and initiation of early somite boundaries. *Nat. Genet.* **19**, 274-278.

Lijam, N. and Sussman, D. (1996). Organization and promoter analysis of the mosue Disheveled-1 gene. *Genome Res*. **5**, 116-124.

Lijam, N., Paylor, R., McDonald, M. P., Crawley, J. N., Deng, C. X., Herrup, K., Stevens, K. E., Maccaferri, G., McBain, C. J., Sussman, D. J. and Wynshaw-Boris, A. (1997). Social interaction and sensorimotor gating abnormalities in mice lacking Dvl1. *Cell* **90**, 895-905.

Lin, Q., Schwartz, J., Bucana, C. and Olsen, E. N. (1997). Control of mouse cardiac morphogenesis and myogenesis by transcriptioin factor MEF2C. *Science* **276**, 1404-1407.

Luo, Z. G., Qiang Wang, Q., Zhou, J. Z., Wang, J., Liu, M. Y., He, X., Wynshaw-Boris, A., Xiong, W. C., Lu, B. and Mei, L. (2002). Dishevelled mediates AChR clustering by interacting with MuSK and PAK1. *Neuron* (in press).

Lyons, I., Parsons, L. M. and Hartley, L. (1995). Myogenic and morphogenetic defects in the heart tubes of muring embryos lacking the nomeobox gene Nkx2.5. *Genes Dev.* **9**, 1654-1666.

Marvin, M. J., DiRocco, G., Gardiner, A., Bush, S. and Lassar, A. B. (2001). Inhibition of Wnt activity induces heart formation from posterior mesoderm. *Genes Dev*. **15**, 316-327.

McLeod, M. J. (1980) Differential staining of carilage and bone in whole mouse fetuses by alcian blue and alizarin red S. *Teratology* **22**, 299-301.

McMahon, A. P. and Bradley, A. (1990). The wnt-1 (Int-1) proto-oncogense is required for development of a large region of the mouse brain. *Cell* **62**, 1073-1085.

Moon, R., Brown, J. and Torres, M. (1997). Wnts modulate cell fate and behavior during vertebrate development. *Trends Genet.* **13**, 157-162.

Moriguchi, T., Kawasaki, K., Kamakura, S., Masuyma, N., Yamanaka, H., Matsumoto, K., Kikuchi, A. and Nishida, E. (1999). Distinct domains of mouse dishevelled are responsible for the c-jun N-terminal kinase/stress activated protein kinase activation and the axis formation in vertebrates. *J. Biol. Chem*. **274**, 30957-30962.

Murdoch, J. N., Doudney, K., Paternotte, C., Copp, A. J. and Stanier, P. (2001). Severe neural tube defects in the *loop-tail* mouse result from mutation of *Lpp1*, a novel gene involved in floor plate specification. *Hum. Mol. Genet.* **10**, 2593-2601.

Muskavitch, M. A. (1994). Delta-Notch signaling and Drosophila cell fate choice. *Dev. Biol*. **166**, 415-430.

Olson, E. and Srivastava, D. (1996). Molecular pathways controlling heart development. *Science* **272**, 671-676.

Perrimon, N. and Mahowald, A. P. (1987). Multiple functions of segment polarity genes in Drosophila. *Dev. Biol*. **119**, 507-600.

Ponting, C., Phillips, C., Davies, K. and Blake, D. (1997). PDZ domains: targeting signaling molecules to sub-membraneous sites. *BioEssays* **19**, 469-479.

Schneider, V. and Mercola, M. (2001). Wnt antagonism initiates cardiogenesis in Xenopus laevis. *Genes Dev*. **15**, 304-315.

Semenov, M. V. and Snyder, M. (1997). Human dishevelled genes constitute a DHR-containing multigene family. *Genomics* **42**, 302-310.

Smalley, M., Sara, E., Paterson, H., Naylor, S., Cook, D., Jayatilake, H., Fryer, L., Hutchison, L., Fry, M. and Dale, T. (1999). Interaction of axin and dvl-2 proteins regulates Dvl2-stimulated TCF-dependent transcription. *EMBO J.* **18**, 2823-2835.

Srivastava, D. (2000). Congenital heart defects, trapping the culprits. *Circ. Res.* **86**, 917.

Srivastava, D. and Olson, E. N. (2000). A genetic blueprint for cardiac development. *Nature* **407**, 221-226.

Srivastava, D., Cserjesi, P. and Olsen, E. N. (1995). A new subclass of bHLH proteins required for cardiac morphogenesis. *Science* **270**, 1995-1999.

Song, D. H., Sussman, D. J. and Seldin, D. C. (2000). Endogenous protein kinase CK2 participates in Wnt signaling in mammary epithelial cells. *J. Biol. Chem.* **275**, 23790-23797.

Strovel, E. T. and Sussman, D. J. (1999). Transient overexpression of murine dishevelled genes results in apoptotic cell death. *Exp. Cell Res.* **253**, 637-648.

Sussman, D. J., Klingensmith, J., Salinas, P., Adams, P. S., Nusse, R. and Perrimon, N. (1994). Isolation and characterization of a mouse homolog of the Drosophila segment polarity gene dishevelled. *Dev. Biol.* **166**, 73-86.

Takada, S., Stark, K. L., Shea, M. J., Vassialeva, G., McMahon, J. A. and McMahon, A. P. (1994). Wnt 3A regulates somite and tailbud formation in the mouse embryos. *Genes Dev.* **7**, 197-203.

Taylor, J., Abramova, N., Charlton, J. and Adler, P. N. (1998). *Van Gogh*: a new *Drosophila* tissue polarity gene. *Genetics* **150**, 199-210.

Thomas, T., Yamagishi, H., Overbeek, P. A., Olsen, E. N. and Srivastava, D. (1998). The bHLH factors, dHAND and eHAND, specify pulmonary and sustemic cardiac ventricles independent of left-right sidedness. *Dev. Biol.* **196**, 228-236.

Thomas, K. and Capecchi, M. (1990). Targeted disruption of the murine int-1 proto-oncogene resulting in severe abnormalities in midbrain and cerebellar development. *Nature* **346**, 847-850.

Theisen, H., Purcell, J., Bennet, M., Kansagara, D., Syed, A. and Marsh, L. J. (1994). *Dishevelled* is required during wingless signaling to establish both cell polarity and cell identity. *Development* **120**, 347-360.

Tsang, M., Lijam, N., Yang, Y., Beier, D. R., Wynshaw-Boris, A. and Sussman, D. J. (1996). Isolation and characterizaation of mouse *Dishevlled-3*. *Dev. Dyn.* **207**, 253-262.

Tybulewicz, V., Crawford, C. E., Jackson, P. K., Bronson, R. T. and Mulligan, R. C. (1991). Neonatal lethality and lymphopenia in mice with a homozygous disruption of the *c-abl* proto-oncogene. *Cell* **65**, 1153-1163.

Wallingford, J. B. and Harland, R. M. (2001). Xenopus Dishevelled signaling regulates both neural and mesodermal convergent extension: parallel forces elongating the body axis. *Development* **128**, 2581-2592.

Wallingford, J. B. and Harland, R. M. (2002). Neural tube closure requires Dishevelled-dependent convergent extension of the midline. *Development* **129**, 5815-5825.

Wallingford, J. B., Rowning, B. A., Vogeli, K. M., Rothbacher, U., Fraser, S. E. and Harland, R. M. (2000). Dishevelled controls cell polarity during Xenopus gastrulation. *Nature* **405**, 81-85.

Wilkinson, D. G. (1992). Whole mount in situ hybridization of vertebrate embryos. In *In Situ Hybridization: A Practical Approach* (ed. D. G. Wilkinson), pp. 75-83. Oxford: IRL Press.

Wolff, T. and Rubin, G. M. (1998). *Strabismus*, a novel gene that regulates tissue polarity and cell fate decisions in *Drosophila*. *Development* **125**, 1149-1159.

Yamaguchi, T., Takada, S., Yoshikawa, Y., Wu, N. and McMahon, A. (1999). T(Brachyury) is a direct target of Wnt3A during paraxial mesoderm specification. *Genes Dev.* **13**, 3185-3190.

Yang, Y., Lijam, N., Sussman, D. J. and Tsang, M. (1996). Genomic organization of mouse *Dishevelled* genes. *Gene* **180**, 121.

Zeng, L., Fagotto, F., Zhang, T., Hsu, W., Vasicek, T. J., Perry, W. L., Lee, J. J., Tilghman, S. M., Gumbiner, B. M. and Costantini, F. (1997). The mouse Fused locus encodes axin, an inhibitor of the Wnt signaling pathways that regulates embryonic axis formation. *Cell* **90**, 181-192.

Zhang, N. and Gridley, T. (1998). Defects in somite formation in lunatic fringe deficient mice. *Nature* **394**, 374-376.